In vivo detection of hemoglobin oxygen saturation and carboxyhemoglobin saturation with multiwavelength photoacoustic microscopy

Zhongjiang Chen, Sihua Yang, and Da Xing*

MOE Key Laboratory of Laser Life Science and Institute of Laser Life Science, College of Biophotonics, South China Normal University, Guangzhou 510631, China

**Corresponding author: xingda@scnu.edu.cn*

Received March 19, 2012; revised July 1, 2012; accepted July 12, 2012; posted July 13, 2012 (Doc. ID 165106); published August 8, 2012

A method for noninvasively detecting hemoglobin oxygen saturation (SO_2) and carboxyhemoglobin saturation (SCO) in subcutaneous microvasculature with multiwavelength photoacoustic microscopy is presented. Blood samples mixed with different concentrations of carboxyhemoglobin were used to test the feasibility and accuracy of photoacoustic microscopy compared with the blood-gas analyzer. Moreover, fixed-point detection of SO_2 and SCO in mouse ear was obtained, and the changes from normoxia to carbon monoxide hypoxia were dynamically monitored *in vivo*. Experimental results demonstrate that multiwavelength photoacoustic microscopy can detect SO_2 and SCO, which has future potential clinical applications.

OCIS codes: 170.1470, 110.5120, 170.2655.

Hemoglobin oxygen saturation is an important physiology index in clinical diagnosis, which can reflect the function of tissues and provide the oxygenation information of microcirculation [1–3]. Carboxyhemoglobin (HbCO) saturation is another important physiology index in carbon monoxide (CO) poisoning. CO poisoning can lead to cerebral hypoxia, brain tissue necrosis, and cranial nerve lesions. Moreover, atherosclerotic cardiovascular disease may be adversely affected by low concentrations of carboxyhemoglobin [4,5]. The blood-gas analyzer is widely used to measure the SO_2 and SCO in clinic. However, it is invasive due to drawing blood before measurement, and the blood-gas analyzer cannot be used to measure SO_2 and SCO dynamically. Though pulse co-oximetry can detect SO_2 and SCO, the low spatial resolution limits its application. Therefore, a method for noninvasively measuring the oxygenations and carboxyhemoglobin in artery and vein is critical in cardiology, oncology, and emergency medicine.

Photoacoustic microscopy (PAM) is a high-resolution and high-contrast noninvasive imaging modality that images optical absorption contrast based on the PA effect [6–8]. PAM has been applied in the imaging of subcutaneous microvasculature, brain functional imaging, and early detection of tumors [9]. In addition, PAM has been used to detect and monitor the blood oxygenation of vessels, which can provide high sensitivity and high specificity [10,11]. In this Letter, we successfully achieve to use PAM to detect SO_2 and SCO in single subcutaneous vessels *in vivo*.

PAM estimation of SO_2 and SCO is similar to near-infrared spectroscopy measurement of SO_2. In CO poisoning, the deoxyhemoglobin (Hb), oxyhemoglobin (HbO_2), and carboxyhemoglobin are treated as the dominant absorbing compounds at each wavelength. Thus, the blood absorption coefficient $\mu_a(\lambda_i)$ (cm^{-1}) through the Lambert–Beer law can be expressed as [11–13]

$$\mu_a(\lambda_i) = \varepsilon_{\mathrm{Hb}}(\lambda_i)[\mathrm{Hb}] + \varepsilon_{\mathrm{HbO_2}}(\lambda_i)[\mathrm{HbO_2}] + \varepsilon_{\mathrm{HbCO}}(\lambda_i)[\mathrm{HbCO}], \quad (1)$$

where $\varepsilon_{\mathrm{Hb}}(\lambda_i)$, $\varepsilon_{\mathrm{HbO_2}}(\lambda_i)$ and $\varepsilon_{\mathrm{HbCO}}(\lambda_i)$ are the known molar extinction coefficients of Hb, HbO_2, and HbCO at wavelength λ_i, respectively, [Hb], [HbO_2], and [HbCO] are the concentrations of each hemoglobin, respectively. Because the amplitude of the acquired localized PA signal $p(\lambda_i, \mathbf{r})$ is proportional to the absorption coefficient $\mu_a(\lambda_i)$ of the absorbers we can replace $\mu_a(\lambda_i)$ by $p(\lambda_i, \mathbf{r})$ to calculate the [Hb], [HbO_2], and [HbCO] [14–17]:

$$\begin{bmatrix} [\mathrm{Hb}] \\ [\mathrm{HbO_2}] \\ [\mathrm{HbCO}] \end{bmatrix}_{(\mathbf{r})} = E^{-1}P(\mathbf{r})K, \quad (2)$$

where

$$P(\mathbf{r}) = \begin{bmatrix} p(\lambda_1, \mathbf{r}) \\ \vdots \\ p(\lambda_n, \mathbf{r}) \end{bmatrix},$$

$$E = \begin{bmatrix} \varepsilon_{\mathrm{Hb}}(\lambda_1) & \varepsilon_{\mathrm{HbO_2}}(\lambda_1) & \varepsilon_{\mathrm{HbCO}}(\lambda_1) \\ \vdots & \vdots & \vdots \\ \varepsilon_{\mathrm{Hb}}(\lambda_n) & \varepsilon_{\mathrm{HbO_2}}(\lambda_n) & \varepsilon_{\mathrm{HbCO}}(\lambda_n) \end{bmatrix}.$$

K is the proportionality coefficient that is related to incident light intensity and the PA signal magnitude, assumed to be wavelength independent. Then SO_2 and SCO are calculated as

$$\mathrm{SO_2} = \frac{[\mathrm{HbO_2}]}{[\mathrm{Hb}] + [\mathrm{HbO_2}] + [\mathrm{HbCO}]},$$
$$\mathrm{SCO} = \frac{[\mathrm{HbCO}]}{[\mathrm{Hb}] + [\mathrm{HbO_2}] + [\mathrm{HbCO}]}. \quad (3)$$

The schematic of the experimental setup is shown in Fig. 1. An optical parametric oscillator (OPO) laser (VIBRANT B 532I, OPOTEK) provides irradiation pulses to excite intrinsic PA signals. The laser has a full width at

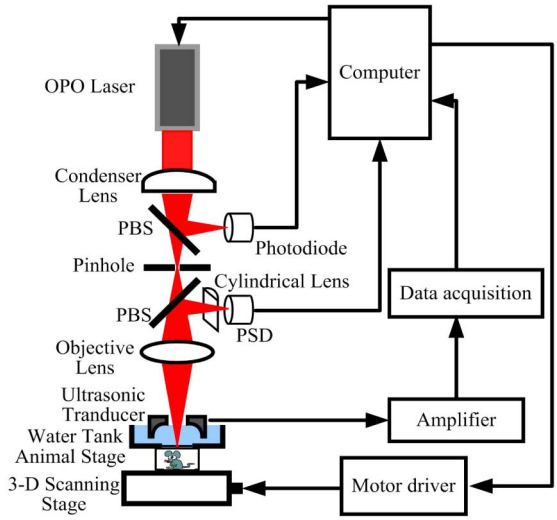

Fig. 1. (Color online) Scheme of the *in vivo* PAM system. The diameter of the pinhole is 100 μm.

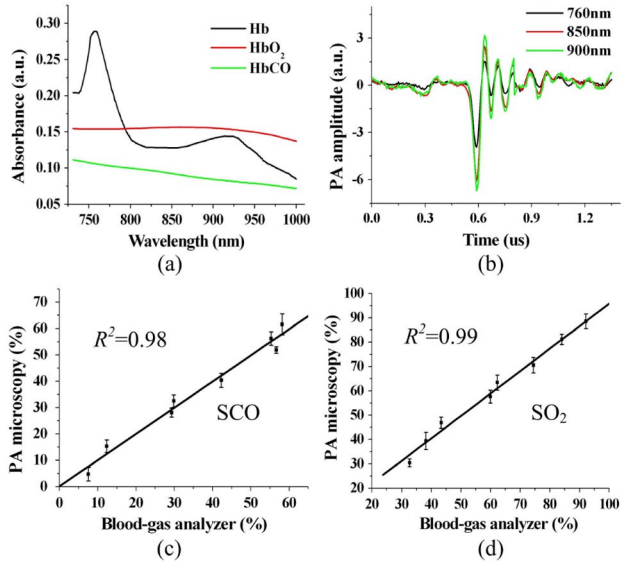

Fig. 2. (Color online) (a) Absorption spectra of the three hemoglobin species: Hb, HbO_2, and HbCO; (b) The PA signals of *in vitro* blood sample at 70.54% SO_2 and 28.1% SCO level. Comparison of the PAM measurements with the blood-gas analyzer measurements of (c) SCO and (d) SO_2 *in vitro* mouse blood samples.

half-maximum of 10 ns and the repetition rate of the laser is 10 Hz. The tuning range of the OPO ranged from 680 to 950 nm. A custom-made 1–3 piezocomposite hollow-focused ultrasound (focus length 5 mm) transducer (Doppler Electronic Technologies Co., Ltd., China) with center frequency of 15 MHz and −6 dB bandwidth of 100% was used to receive the PA signals. The laser beam was focused by an objective lens (NA 0.1; WD 37.5 mm) through the small hole (diameter 2 mm) in the center of the hollow sensor. A data acquisition card (NI5124, National Instruments) received the amplified PA signals from the hollow sensor at a sampling rate of 200 M samples/s. A three-dimensional scanning stage was driven by computer-controlled stepper motors (MC600AS, Zolix). A silicon photodiode was used to monitor and calibrate the intensity and stability of the laser beam. The cylindrical lens and the position sensor device (PSD) comprised an auto focusing system.

In order to verify the feasibility of the PAM system detecting SO_2 and SCO, blood samples were tested *in vitro*, as shown in Fig. 2. Venous mouse blood was freshly collected and mixed with anticoagulant. Eight samples of mouse blood containing various amounts of CO were prepared. The samples were measured by a blood-gas analyzer (Rapidpoint 405, Siemens) as control prior to PA measurement. The Hb, HbO_2, and HbCO from mouse blood were obtained, and then their absorption spectra were measured with a spectrometer (Lambda 35, Perkin-Elmer, USA). The results are shown in Fig. 2(a). Three wavelengths (760, 850, 900 nm) were used in all of our experiments. Figure 2(b) shows the detected PA signals at the three wavelengths for the sample at 70.54% SO_2 and 28.1% SCO level. According to Eqs. (2) and (3), the PA signals of different SO_2 and SCO levels are proportional to the absorptions of each blood sample, respectively. The levels of SO_2 and SCO in different samples were calculated using the peak of PA signals; measurements were repeated 100 times per sample. PA measurement results matched well with the results of the blood-gas analyzer [Figs. 2(c) and 2(d)]. The above results demonstrate that PAM can reliably and accurately measure the levels of SO_2 and SCO *in vitro*.

In the *in vivo* study, the data were acquired on a BALB/c mouse (35 g) ear. The hair was removed from the ear with commercial hair remover (Payven Depilatory China). Sodium pentobarbital (40 mg/kg; supplemental, 10 mg/kg/h) was administered to keep the mouse motionless in the experiment. Two physiological states (normoxia and carbon monoxide hypoxia) were introduced by controlling the time of inhaled mixed-gases (1% CO mixed in the normal air). All experimental animal procedures were carried out in accord with the guidelines of the South China Normal University.

Before the mouse was at the carbon monoxide hypoxia state, the PAM image of the microvasculature in the mouse ear was acquired at 532 nm under normoxia, as shown in Fig. 3(a). Then the mouse inhaled mixed-gases for 10 min, and the two blood vessels across the scan line A were detected at the three wavelengths. The two blood vessels can be easily distinguished in Fig. 3(b). Three colored dotted curves represented the PA signal maximum amplitude projection at three respective wavelengths. In order to detect the levels more precisely, we obtained 100 data points for every vascular position by selecting 20 neighboring data points per scan and performing five scans. Meanwhile, the SCO and SO_2 of vein and artery blood were measured by the blood-gas analyzer. The artery and vein can be separated based on the SCO levels as well as the SO_2 levels, which are physiologically distinct for venous and arterial blood, as shown in Figs. 3(c) and 3(d), respectively. We found an SCO level of 43.21% and 46.72% for the artery and 40.63% and 39.58% for the vein for the PAM measurement and blood-gas analyzer, respectively. The values found for the SO_2 level were 56.53% and 64.46% for the artery and 53.5% and 62.38% for the vein for the PAM measurement and blood-gas analyzer, respectively. The relative error of the PAM measurement of the SCO and SO_2 was 5.1% and 13.1%,

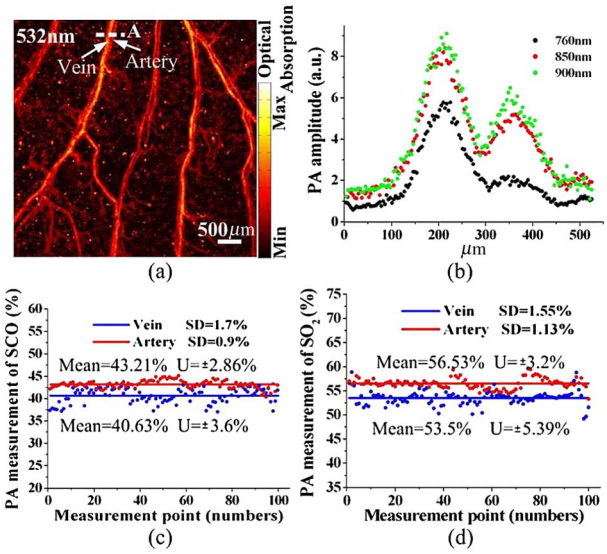

Fig. 3. (Color online) (a) PAM image of microvasculature in a mouse ear at the wavelength of 532 nm under normoxia. The lateral resolution is ~50 μm; (b) The reconstructed profile of the blood vessel obtained at 760, 850, and 900 nm, respectively, at the position indicated by the dashed line in (a). PA measured; (c) SCO; and (d) SO_2 levels of the vein and artery vessels at the position indicated by the dashed line in (a). SD, standard deviation; U, uncertainty.

respectively. The discrepancy presumably came from the wavelength-dependent optical attenuation of the tissue, which could be compensated by a system calibration. In addition, the scanning time (210 s) could also decrease the accuracy of the PAM measurement. The experiment results have confirmed the reliability of PAM for detecting the SCO and SO_2 *in vivo*.

To further verify the ability of PAM to detect variations in SCO and SO_2 at a fixed point, a series of SCO and SO_2 levels at different points in time were acquired, as shown in Fig. 4. The mouse inhaled the mixed-gases at 5 min, and stopped at 15 min. The SCO levels of artery and vein changed from 1.05% to 42.57%, and 1.67% to 40.36% in 10 min, respectively [Fig. 4(a)]. From 15 min to 12 h, the SCO level of the artery and vein continuously recovered close to normal levels. This can be explained by considering that the ability of deoxyhemoglobin binding with the CO is 200 times stronger than that of O_2. Furthermore, the dissociation rate of carboxyhemoglobin is slower than that of oxyhemoglobin [18]. The level of SO_2 from normoxia to carbon monoxide hypoxia is shown in Fig. 4(b). The

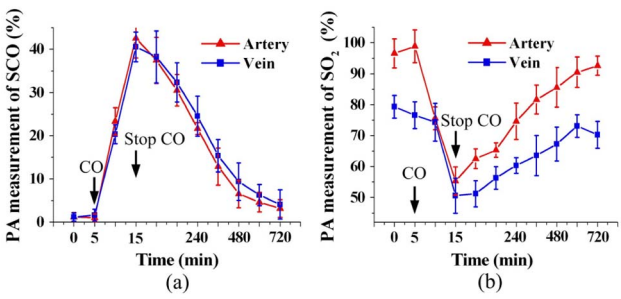

Fig. 4. (Color online) PAM monitoring of (a) SCO and (b) SO_2 level changes in vein and artery of mouse ear from normoxia to carbon monoxide hypoxia.

experiment suggests that PAM has the capacity to monitor changes in the level of SO_2 and SCO over time.

The *in vivo* experiments have demonstrated the ability of PAM for imaging the microvasculature and detecting the level of its SO_2 and SCO, which can contribute to diagnosis and treatment. Generally, the SCO level is a very important physiology index in CO poisoning; the SO_2 level is a supplementary index. Simultaneous measurement of the two indexes can make the diagnosis more accurate. In addition, the accuracy of the PAM measurement could be improved by using a high repetition rate laser and compensating the optical attenuation in the tissue.

In summary, we have proposed a method for noninvasive detection of SO_2 and SCO using a PAM system. In the present study, PAM was used to image the microvasculature of the mouse ear and detect SO_2 and SCO *in vivo* under continuous change of various physiological states with high resolution. Therefore, PAM can be used to diagnose carbon monoxide poisoning and prognosis, which has great potential application to detect SO_2 and SCO in clinic.

This research is supported by the National Basic Research Program of China (2011CB910402; 2010CB732602), the Program for Changjiang Scholars and Innovative Research Team in University (IRT0829), and the National Natural Science Foundation of China (81127004, 11104087).

References

1. P. W. McCormick, M. Stewart, M. G. Goetting, and G. Balakrishnan, Stroke **22**, 596 (1991).
2. D. Malonek and A. Grinvad, Science **272**, 551 (1996).
3. A. G. Tsai, P. C. Johnson, and M. Intaglietta, Physiol. Rev. **83**, 933 (2003).
4. E. M. Dwyer and G. M. Turino, N. Engl. J. Med. **321**, 1474 (1989).
5. E. N. Allred, E. R. Bleecker, B. R. Chaitman, T. E. Dahms, S. O. Gottlieb, J. D. Hackney, M. Pagano, R. H. Selvester, S. M. Walden, and J. Warren, N. Engl. J. Med. **321**, 1426 (1989).
6. H. F. Zhang, K. Maslov, G. Stoica, and L. V. Wang, Nat. Biotechnol. **24**, 848 (2006).
7. K. Maslov, G. Stoica, and L. V. Wang, Opt. Lett. **30**, 625 (2005).
8. Y. Yuan, S. H. Yang, and D. Xing, Appl. Phys. Lett. **100**, 023702 (2012).
9. X. Wang, Y. Pang, G. Ku, X. Xie, G. Stoica, and L. V. Wang, Nat. Biotechnol. **21**, 803 (2003).
10. I. Y. Petrov, Y. Petrov, D. S. Prough, D. J. Deyo, I. Cicenaite, and R. O. Esenaliev, Biomed. Opt. Express **3**, 125 (2012).
11. H. F. Zhang, K. Maslov, M. Sivaramakrishnan, G. Stoica, and L. V. Wang, Appl. Phys. Lett. **90**, 053901 (2007).
12. Y. Wang, S. Hu, K. Maslov, Y. Zhang, Y. Xia, and L. V. Wang, Opt. Lett. **36**, 1029 (2011).
13. T. Jetzfellner, A. Rosenthal, A. Buehler, K. Englmeier, D. Razansky, and V. Ntziachristos, Opt. Lett. **36**, 4176 (2011).
14. B. Chance, E. Borer, A. Evans, G. Holtom, J. Kent, M. Maris, K. Mccully, J. Northrop, and M. Shinkwin, Ann. N.Y. Acad. Sci. **551**, 1 (1988).
15. J. Laufer, C. Elwell, D. Delpy, and P. Beard, Proc. SPIE **6086**, 60861J (2006).
16. R. Ma, A. Taruttis, V. Ntziachristos, and D. Razansky, Opt. Express **17**, 21414 (2009).
17. G. Z. Yin, D. Xing, and S. H. Yang, J. Appl. Phys. **106**, 013109 (2009).
18. J. Varon, P. E. Marik, R. E. Fromm, Jr., and A. Gueler, J. Emerg. Med. **17**, 87 (1999).